Human copper transporter 2 is localized in late endosomes and lysosomes and facilitates cellular copper uptake

Peter V. E. VAN DEN BERGHE*, Dineke E. FOLMER*, Helga E. M. MALINGRÉ*, Ellen VAN BEURDEN*, Adriana E. M. KLOMP*, Bart VAN DE SLUIS*†, Maarten MERKX‡, Ruud BERGER* and Leo W. J. KLOMP*[1]

*Department of Metabolic and Endocrine Diseases, University Medical Center Utrecht, 3584 EA Utrecht, The Netherlands, †Complex Genetics Section, Department of Medical Genetics, University Medical Center Utrecht, 3508 TA Utrecht, The Netherlands, and ‡Department of Biomedical Engineering, Technical University Eindhoven, 5600 MB Eindhoven, The Netherlands

High-affinity cellular copper uptake is mediated by the CTR (copper transporter) 1 family of proteins. The highly homologous hCTR (human CTR) 2 protein has been identified, but its function in copper uptake is currently unknown. To characterize the role of hCTR2 in copper homoeostasis, epitope-tagged hCTR2 was transiently expressed in different cell lines. hCTR2–vsvG (vesicular-stomatitis-virus glycoprotein) predominantly migrated as a 17 kDa protein after imunoblot analysis, consistent with its predicted molecular mass. Chemical cross-linking resulted in the detection of higher-molecular-mass complexes containing hCTR2–vsvG. Furthermore, hCTR2–vsvG was co-immunoprecipitated with hCTR2–FLAG, suggesting that hCTR2 can form multimers, like hCTR1. Transiently transfected hCTR2–eGFP (enhanced green fluorescent protein) was localized exclusively to late endosomes and lysosomes, and was not detected at the plasma membrane. To functionally address the role of hCTR2 in copper metabolism, a novel transcription-based copper sensor was developed. This MRE (metal-responsive element)–luciferase reporter contained four MREs from the mouse metallothionein 1A promoter upstream of the firefly luciferase open reading frame. Thus the MRE–luciferase reporter measured bioavailable cytosolic copper. Expression of hCTR1 resulted in strong activation of the reporter, with maximal induction at 1 μM $CuCl_2$, consistent with the K_m of hCTR1. Interestingly, expression of hCTR2 significantly induced MRE–luciferase reporter activation in a copper-dependent manner at 40 and 100 μM $CuCl_2$. Taken together, these results identify hCTR2 as an oligomeric membrane protein localized in lysosomes, which stimulates copper delivery to the cytosol of human cells at relatively high copper concentrations. This work suggests a role for endosomal and lysosomal copper pools in the maintenance of cellular copper homoeostasis.

Key words: copper biosensor, copper transporter 1 (Ctr1), copper transporter 2 (Ctr2), copper uptake, metallothionein, zinc.

INTRODUCTION

Copper is a trace element which is essential for all organisms that utilize oxygen as an electron acceptor during respiration. As a transition metal, copper serves as a cofactor in a number of redox enzymes. The same redox-active properties also render the metal potentially toxic, as it can induce free radical formation and cause direct damage to proteins, lipids and DNA. To maintain copper homoeostasis, remarkably efficient mechanisms have evolved to regulate copper import and export and cellular distribution of the metal. The proteins involved in cellular copper homoeostasis are largely conserved in both prokaryotes and eukaryotes [1–3]. These proteins form intricate metabolic pathways aimed at maintaining an extremely low free copper concentration, while ensuring that sufficient copper is bioavailable to sustain essential copper-dependent cellular processes [4]. As one example, a significant proportion of cellular copper is bound to copper chaperones, which deliver copper to specific target enzymes or transporters by regulated protein–protein interactions [5,6]. A second example, metallothioneins are small ubiquitously expressed proteins that scavenge cytosolic copper and other metals such as zinc and cadmium [7], and the expression of metallothionein genes is transcriptionally regulated in a copper-dependent fashion.

Severe disorders may arise as a result of disruption of copper homoeostasis. Recessive mutations in the gene encoding ATP7A (copper-transporting P_{1B}-type ATPase) result in Menkes disease, a fatal X-linked neurodevelopmental disorder [8,9]. ATP7A deficiency results in a lack of copper transport through the placenta and the intestinal epithelium, leading to systemic copper deficiency and the failure to provide essential cuproenzymes with the metal. The *calamity* mutant of *Danio rerio*, the zebrafish, is a recently characterized animal model for Menkes disease [10], which displays a marked reduction in pigment formation and a strikingly altered notochord development in comparison with wild-type zebrafish. Interestingly, the *calamity* mutant is phenocopied by copper deficiency, thus illustrating further the essential role of copper in physiology and development.

Copper uptake is facilitated by the CTR (copper transporter) family of proteins, which are highly conserved [11]. In *Saccharomyces cerevisiae*, high-affinity uptake of copper is mediated by yCtr1p and yCtr3p [12,13]. A third Ctr protein expressed in *S. cerevisiae*, yCtr2p, is thought to mediate low-affinity copper uptake. In mammals, a high-affinity copper permease, CTR1, facilitates copper import, with a K_m of approx. 1–5 μM [14]. hCTR (human CTR) 1 is predominantly localized to intracellular vesicles which are in close apposition to the Golgi

Abbreviations used: ATP7A, copper-transporting P_{1B}-type ATPase; BCS, bathocuproinedisulfonic acid; CTR, copper transporter; DFO, desferrioxamine; DMEM, Dulbecco's modified Eagle's medium; eGFP, enhanced green fluorescent protein; EGS, ethylene glycolbis(succinimidylsuccinate); FCS, foetal calf serum; hCTR, human CTR; HEK-293T cell, human embryonic kidney cell expressing the large T-antigen of SV40 (simian virus 40); LAMP, lysosome-associated membrane protein; MEF, mouse embryonic fibroblast; MRE, metal-responsive element; MTF, metal responsive transcription factor; MTT, 3-(4,5-dimethylthiazol-2-yl)-2,5-diphenyl-2*H*-tetrazolium bromide; RLU, relative light units; TfR, transferrin receptor; TGN, *trans*-Golgi network; vsvG, vesicular-stomatitis-virus glycoprotein.

[1] To whom correspondence should be addressed (email L.Klomp@umcutrecht.nl).

complex, but a fraction is also present at the plasma membrane [15,16]. The proportion of cell-surface-exposed hCTR1 is dependent on the cell type [15], and elevated concentrations of copper have been shown to result in the internalization of cell-surface hCTR1, possibly as a rapid adaptive response to limit copper uptake [17]. hCTR1 contains three membrane-spanning regions and is thought to assemble into a trimer which forms an aqueous pore to enable copper transport [18,19].

The physiological role of the Ctr1 family of proteins has been addressed elegantly using knockout mouse models. *Ctr1*-knockout mice died during mid-gestation as a result of copper deficiency [20,21]. Conditional knockout mice, lacking *Ctr1* specifically in the intestinal epithelium, were born healthy, but displayed markedly impaired dietary copper uptake, resulting in a severe systemic copper deficiency comparable with Menkes disease patients [22]. This knockout mouse work established the essential role of Ctr1 in embryonic development and in dietary copper uptake. However, these animals display some residual cellular copper uptake, suggesting that additional pathways of copper import do exist. Furthermore, MEFs (mouse embryonic fibroblasts) obtained from *Ctr1*-knockout embryos survived in culture without the addition of extra copper to their medium, and were able to take up copper in a low-affinity manner [23]. The proteins mediating Ctr1-independent low-affinity copper import have currently not been characterized.

A candidate protein which may participate in such alternative copper import routes is hCTR2. Alignment of the primary amino acid sequences of hCTR1 and CTR2 from multiple species revealed marked homology in the transmembrane regions, suggesting that hCTR2 contains three putative transmembrane regions, similar to hCTR1 [14,24] (Figure 1A). Extrapolating from hCTR1, the N-terminus of hCTR2 is probably located extracytoplasmically [14,24]. The highly conserved MXXXM (Met-Xaa-Xaa-Xaa-Met) motif in the second transmembrane region of hCTR1, which has been shown to be critical for copper coordination during copper uptake [25], is also present in hCTR2. All amino acid residues that have been shown to be critical for oligomerization and copper transport activity of hCTR1 are conserved in hCTR2: the GXXXG (Gly-Xaa-Xaa-Xaa-Gly) motif in the third putative transmembrane region of hCTR1 [26], one methionine residue, approx. 20 residues upstream of the first transmembrane domain (Figure 1A), and the MXXXM motif in the second transmembrane domain [27]. There are also notable differences between hCTR2 and hCTR1. hCTR2 lacks the MXXXM motif and histidine-rich regions that are important for high-affinity copper transport, and does not contain the appropriate consensus sites for N-glycosylation [27–29]. These observations support the hypothesis that hCTR2 does transport copper, but suggest that this occurs with a lower affinity than that of hCTR1. However, the function of hCTR2 has not been experimentally addressed and its annotation as a CTR has been based only on the alignment with other CTR sequences [30]. In the present study, we have characterized the role of hCTR2 in copper homoeostasis using a combination of biochemical analyses, cellular localization studies and a novel copper sensor. The results provide evidence that hCTR2 is an intracellular protein involved in copper uptake in human cells.

EXPERIMENTAL

Cell culture and MTT [3-(4,5-dimethylthiazol-2-yl)-2,5-diphenyl-2*H*-tetrazolium bromide] viability assay

The HEK-293T cell [human embryonic kidney cell expressing the large T-antigen of SV40 (simian virus 40)] line, HeLa cell line and U2OS cell line were purchased from the A.T.C.C. Cells were cultured at 37 °C under humidified air containing 5 % CO_2, and were maintained in DMEM (Dulbecco's modified Eagle's medium) GlutaMAX™ (Invitrogen) containing 10 % (v/v) FCS (foetal calf serum) (Invitrogen), 100 μg/ml penicillin (Invitrogen) and 100 μg/ml streptomycin (Invitrogen). For some experiments, cells were cultured in DMEM containing 10 % FCS, 100 μg/ml penicillin and 100 μg/ml streptomycin in the presence of different concentrations of $CuCl_2$, $ZnCl_2$, $MgCl_2$, $FeCl_3$, $MnCl_2$ (Merck Chemicals) or a copper chelator, BCS (bathocuproinedisulfonic acid) (Sigma). MTT viability assays [31] were performed after incubation of the cells with different concentrations of metals in 96-well microtitre plates (Corning). Cells were incubated with 0.4 mg/ml MTT (Sigma) in DMEM containing 10 % (v/v) FCS, 100 μg/ml penicillin and 100 μg/ml streptomycin for 30 min at 37 °C. Prior to lysis, cells were rinsed twice with PBS (25 mM sodium phosphate buffer and 140 mM NaCl, pH 7.4) and lysed in 100 μl of 100 % propan-2-ol containing 40 mM HCl. Conversion of MTT into formazan was measured at 595 nm using a multi-plate reader model 550 spectrophotometer (Bio-Rad), and the viability of the cells was calculated relative to untreated cells.

Plasmids

pCL-NEO RabIP4-vsvG (vesicular-stomatitis-virus glycoprotein) was kindly provided by Dr P. J. van de Sluijs (Department of Cell Biology, University Medical Center Utrecht, Utrecht, The Netherlands). pcDNA3.1-cullin1-FLAG was amplified from liver cDNA using FLAG–cullin forward and reverse primers (Table 1). The PCR fragment was cloned into pCRII (Invitrogen) and subsequently cloned into pcDNA3.1/ZEO. hCTR2–vsvG cDNA was amplified from cDNA by PCR using hCTR2–vsvG forward and hCTR2–vsvG reverse primers, and subsequently subcloned into pZeoSV2. The reverse primer contained a sequence to add the vsvG tag at the C-terminus of hCTR2 as described previously for hCTR1–vsvG [15]. To construct pcDNA3.1/Zeo-hCTR1-vsvG (hCTR1–vsvG) and pcDNA3.1/Zeo-hCTR2-vsvG (hCTR2–vsvG), hCTR1–vsvG and hCTR2–vsvG fragments were isolated from pZeoV2-hCTR1-vsvG [15] or pZeoV2-hCTR2-vsvG after digestion with BamHI and XbaI. The fragments were ligated into the BamHI and XbaI sites of pcDNA3.1/Zeo (Invitrogen). To generate C-terminal eGFP (enhanced green fluorescent protein)-tagged hCTR1 and hCTR2, hCTR1 and hCTR2 fragments were amplified from cDNA by PCR using the Advantage cDNA polymerase mix (Clontech), with hCTR1 and hCTR2 forward and reverse primers respectively (Table 1). The fragments were ligated into the pCRII vector using the TA-cloning kit (Invitrogen). hCTR1 and hCTR2 fragments were isolated from pCRII after EcoRI digestion and subsequently cloned into the EcoRI site of pEGFP-N3 (Clontech), resulting in peGFP-N3-hCTR1 (hCTR1–eGFP) and peGFP-N3-hCTR2 (hCTR2–eGFP). To generate the pGL3-E1b-TATA-4MRE construct [MRE (metal-responsive element)–luciferase reporter], four MREs were amplified by PCR from the 4 × MRE(d) construct [7,32] using 4MRE-F/HindIII and 4MRE-R/PstI primers (Table 1). The fragment was digested by HindIII and PstI, and subsequently subcloned into the E1b-TATA pGL3 vector (kindly provided by Dr Eric Kalkhoven, University Medical Centre Utrecht, Utrecht, The Netherlands). hCTR1 and hCTR2 constructs with a C-terminal FLAG tag were generated by PCR of hCTR1–vsvG and hCTR2–vsvG template constructs using Pfu Turbo polymerase (Stratagene) and the corresponding BamHI forward and NotI reverse primers for hCTR1 and hCTR2 respectively. These PCR fragments were digested with BamHI and NotI,

Table 1 Primers

fw, forward; rev, reverse.

Name	Sequence (5′ → 3′)
FLAG–cullin1 rev	tcacttgtcgtcatcgtcttgtagtcagccaagtaactgtaggtgtc
FLAG–cullin1 fw	atggactacaaagacgatgacgacaagtcgtcaacccggagccag
hCTR2–vsvG fw	atggcgatgcatttcatctt
hCTR2–vsvG rev	tcactttcctagtcggttcatctcgatgtcagtgtaagctgtgctgagaagtgg
hCTR1 fw	tggatcattcccaccatatg
hCTR1 rev	atgggcaatgctctgtgatatc
hCTR2 fw	atggcgatgcatttcatctt
hCTR2 rev	agctgtgctgagaagtgggt
4MRE-F/HindIII	cccaagcttgactcgaggagctctgcac
4MRE-R/PstI	ctgcagtatgccaaggtcgacgggc
hCTR2 BamHI fw	ctaggatccaccatggcgatgcatttcatcttc
hCTR2 NotI rev	gtaagcggccgcagctgtgctgagaagtgggtaag
hCTR1 BamHI fw	ggatccgccaccatggatcattcccaccatatg
hCTR1 NotI rev	gcggccgcatggcaatgctctgtgatatc
hCTR1 IXXXI fw	cataagctacttcctcattctcatcttcattacctacaacgggtac
hCTR1 IXXXI rev	gtacccgttgtaggtaatgaagatgagaatgaggaagtagcttatg
hCTR2 IXXXI fw	catcggctacttcatcattctggccgtaatttcctacaacacctg
hCTR2 IXXXI fw	caggtgttgtaggaaattacggccagaatgatgaagtagccgatg

and the fragments were ligated into the BamHI and NotI sites in pEBB-FLAG (kindly provided by Dr C.S. Duckett, University of Michigan Medical School, Ann Arbor, MI, U.S.A.), resulting in pEBB-hCTR1-FLAG and pEBB-hCTR2-FLAG constructs. pEBB-hCTR1-FLAG IXXXI (Ile-Xaa-Xaa-Xaa-Ile) and pEBB-hCTR2-FLAG IXXXI were generated by QuikChange® site-directed mutagenesis (Stratagene), using the hCTR1 IXXXI forward and reverse primers and the hCTR2 IXXXI forward and reverse primers. All constructs were verified by sequence analysis.

Transfection, chemical cross-linking, immunoprecipitation and immunoblot analysis

HEK-293T cells were transiently transfected with either hCTR1–vsvG or hCTR2–vsvG using the calcium phosphate precipitation protocol [33]. DNA was diluted to a maximum concentration of 10 μg/ml in 244 mM $CaCl_2$ solution. The DNA mixture was then diluted with an equal volume of 2 × HBSS (to a final concentration of 6.275 mM Hepes, 190 μM Na_2HPO_4, 68.5 mM NaCl and 122 mM $CaCl_2$, pH 7.5). After incubating for 20 min at 20 °C, the transfection mixture was added to the cells in 10 ml DMEM, and the cells were harvested after 2 days. Chemical cross-linking was performed by incubation of transfected HEK-293T cells for 30 min at room temperature (20 °C) with PBS containing 1 % DMSO in 0 mM, 0.5 mM or 1 mM EGS [ethylene glycolbis(succinimidylsuccinate)] (Pierce). For cross-linking experiments and immunoprecipitation, HEK-293T cells were lysed in RIPA buffer [50 mM Tris/HCl, pH 7.4, 0.1 % (v/v) SDS, 1 % (v/v) Nonidet P40, 150 mM NaCl, 10 mg/ml sodiumdeoxychalate, 2 mM EDTA and 1 mM $NaVO_3$] supplemented with Complete™ protease inhibitor cocktail (Roche), and lysates were solubilized by passage seven times through a needle (23 gauge). For immunoprecipitation, 1 mg of total protein, 20 μl of Protein A–agarose beads (Sigma) and 0.6 μg of rabbit anti-vsvG antibody (Abcam) were incubated overnight at 4 °C in a volume of 500 μl while rotating. For co-immunoprecipitation experiments, 1 ml of the cell lysate was divided into two precipitation reaction mixtures with either 20 μl of Protein A–agarose beads and 0.6 μg of rabbit anti-vsvG antibody or 20 μl of anti-FLAG M2–agarose (Sigma), which were incubated for 4 h at 4 °C with rotation. Immunocomplexes were precipitated by microcentrifugation at 2000 ***g*** for 3 min at 4 °C and washed four times in RIPA buffer. Immunoprecipitates were resuspended in SDS/PAGE sample buffer [62.5 mM Tris/HCl, 4 % (v/v) SDS, 5 % (v/v) glycerol, 0.01 % (w/v) Bromophenol Blue and 2 % (v/v) 2-mercaptoethanol, pH 6.8] and heated at 95 °C for 5 min prior to resolution by SDS/PAGE (12 % gels). Proteins were transferred on to Hybond-P PVDF membranes (Amersham Biosciences) by standard immunoblot procedures. The membranes were blocked in Tris-buffered saline (25 mM Tris/HCl, pH 7.4, 137 mM NaCl and 2.7 mM KCl) containing 5 % (w/v) non-fat dried milk (Sigma) and 0.1 % (v/v) Tween 20. Immunoblots were probed with rabbit anti-vsvG antibody (0.6 μg/ml) (Abcam), mouse anti-(vsvG hybridoma) supernatant from clone P5D4 (1:250 dilution) [24] or horseradish-peroxidase-conjugated mouse anti-FLAG M2 antibody (Sigma) for 1 h. Reactivity was detected using horseradish-peroxidase-conjugated secondary antibodies (1 ng/ml; Pierce) and ECL® (enhanced chemiluminescence) (Amersham Biosciences), according to the manufacturer's instructions.

Indirect immunofluorescence and confocal laser-scanning microscopy

HEK-293T cells, U2OS cells and HeLa cells were transiently transfected with hCTR1–eGFP, hCTR2–eGFP or hCTR2–vsvG, using Lipofectamine™ 2000 (Invitrogen) according to the manufacturer's protocol. At 1 day after transfection, cells were treated with trypsin and seeded on to coverslips (Paul Marienfeld, GmbH & Co.). After 24 h, cells were rinsed with ice-cold PBS and fixed in 3.7 % (w/v) paraformaldehyde in PBS for 20 min at 4 °C. Cells were rinsed three times with 0.02 % (v/v) Triton X-100 in PBS, and non-specific binding was blocked with blocking buffer [5 % (w/v) BSA in PBS and 0.02 % (v/v) Triton X-100] for 30 min at room temperature. Immunolabelling was performed in blocking buffer for 1 h with the antibodies indicated below. Cells were rinsed three times with 0.02 % (v/v) Triton X-100 in PBS, and secondary labelling was performed with affinipure Alexa Fluor® 568-conjugated goat anti-(mouse IgG) or goat anti-(rabbit IgG) antibodies (10 μg/ml; Molecular Probes). Coverslips were mounted in Fluorsave (VWR International), and confocal laser-scanning microscopy was performed using a Leica TCS 4D microscope equipped with a Plan APO ×63 oil immersion objective (numerical aperture 1.4) and dedicated imaging software (Leica TCSNT version 1.6.587). hCTR1–vsvG and hCTR2–vsvG were labelled with rabbit anti-vsvG antibodies (0.6 μg/ml) (Abcam). For double-labelling experiments, monoclonal antibodies against p230 (230 kDa protein) [a TGN (*trans*-Golgi network) marker] (1.25 μg/ml; BD Biosciences), human TfR (transferrin receptor) (1 μg/ml; Molecular Probes), CD63 (a late endosomal marker) (75 ng/ml; Zymed Laboratories) and the lysosomal markers CD107a [LAMP (lysosome-associated membrane protein)-1] and CD107b (LAMP-2) (5 μg/ml; BD Biosciences) were used.

Luciferase reporter assays

For luciferase reporter assays, HEK-293T cells were seeded in 96-well plates and transiently transfected using the calcium phosphate transfection protocol. Each well was co-transfected with 35 ng of the MRE–luciferase reporter, 0.25 ng of pRL-TK vector (Promega Benelux BV) and 3.5 ng of hCTR1–vsvG, 3.5 ng of hCTR2–vsvG, 0.35 ng of pEBB-hCTR1-FLAG or 0.35 ng of pEBB-hCTR2-FLAG constructs as indicated. After incubation for 24 h, the cells were rinsed with PBS and subsequently maintained for 24 h in DMEM in the presence or absence of different metals. To investigate the response to hypoxia,

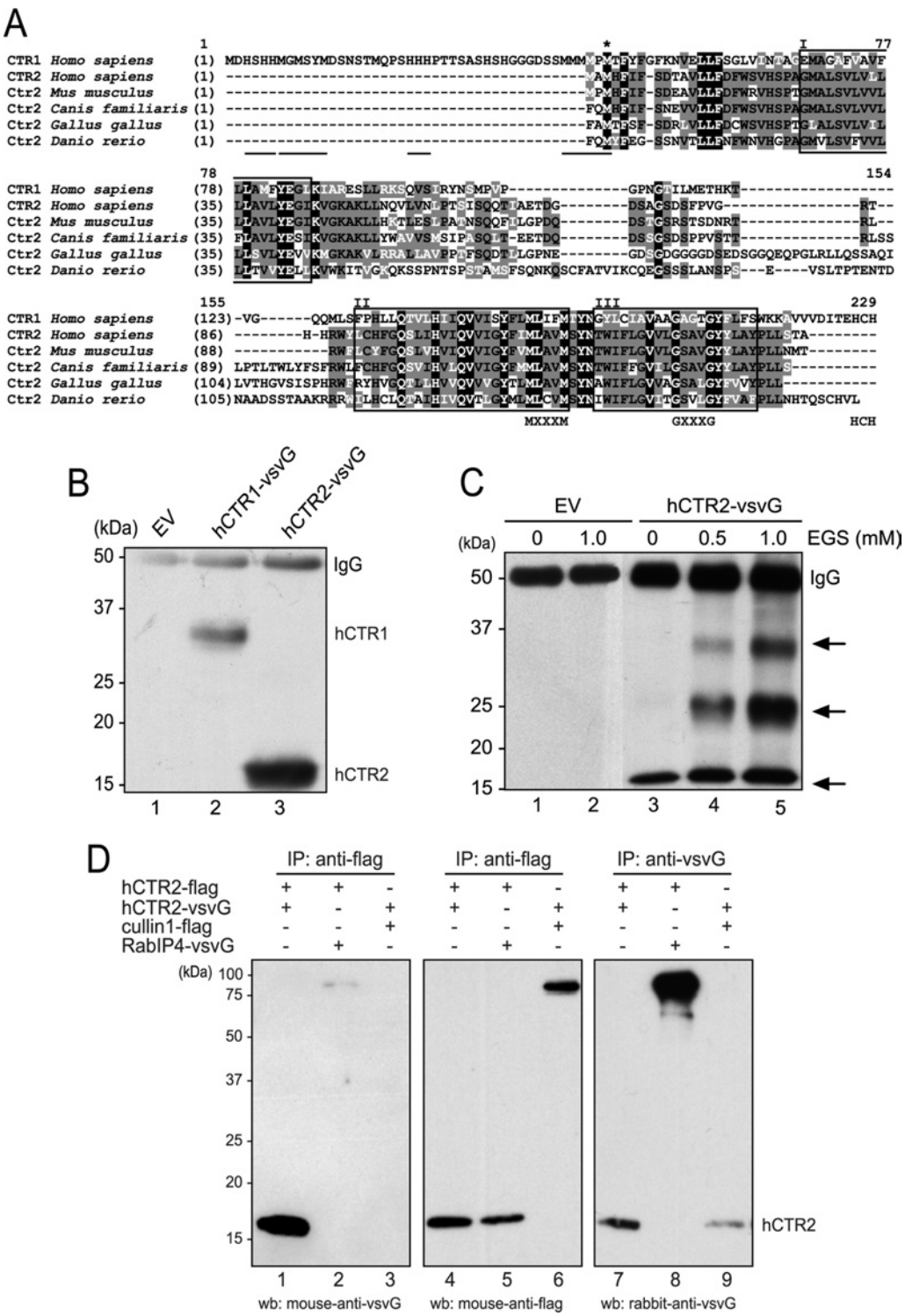

Figure 1 Biochemical characterization of hCTR2

(**A**) Sequence alignment between hCTR1 and CTR2 from different species using the AlignX module from Vector NTI (Invitrogen). Identical regions (white text on black background), conserved regions (black text on grey background) and similar regions (white text on grey background) of amino acids are indicated. The transmembrane regions (boxed regions) are indicated by roman numerals. The MXXXM motif, the GXXXG motif involved in intrahelical interactions and the C-terminal His-Cys-His (HCH) motif are indicated. The methionine motifs and histidine-rich regions involved in high-affinity copper transport are underlined, and one conserved methionine residue is indicated by an asterisk. (**B**) Empty vector (EV), hCTR1–vsvG or hCTR2–vsvG constructs (lanes 1–3) were transiently transfected into HEK-293T cells prior to lysis. Immunoblot analysis was performed on proteins immunoprecipitated by anti-vsvG antibodies. (**C**) HEK-293T cells were transiently transfected with EV (lanes 1 and 2) or hCTR2–vsvG (lanes 3–5) constructs. Cells were incubated for 30 min at room temperature with increasing concentrations of the chemical cross-linker EGS (lanes 2–5). Immunoprecipitation and subsequent immunoblot analysis was performed to detect hCTR2–vsvG-containing complexes (arrows). The heavy chain of the antibodies is indicated (IgG). (**D**) HEK-293T cells were transiently co-transfected with hCTR2–FLAG (flag), hCTR2–vsvG, cullin1–FLAG or RABIP4–vsvG. Immunoprecipitation (IP) was performed with either mouse anti-FLAG M2–agarose beads or rabbit anti-vsvG attached to Protein A–agarose beads. Precipitates were washed and resolved by SDS/PAGE (12 % gels), and immunoblot (wb) analysis was performed with antibodies as indicated. Molecular masses in kDa are shown on the left-hand side of the immunoblots.

cells were transiently transfected with 10 ng of the hypoxia-responsive reporter vector with 5× HRE [34] and 0.25 ng of pRL-TK vector. After 24 h, cells were incubated for a further 24 h with 100 μM DFO (desferrioxamine), an iron chelator. After incubation, the cells were rinsed in PBS, harvested in passive lysis buffer (Promega) according to the manufacturer's protocol and assayed by luminometry (Berthold Technologies) using the Dual-Luciferase® reporter assay system (Promega) for firefly luciferase activity and *Renilla* luciferase activity, according to the manufacturer's protocol. The RLU (relative light units) were calculated by dividing firefly luciferase measurements by *Renilla* luciferase measurements. All values were expressed as fold inductions relative to empty vector control incubations (set at 1). Statistical analysis was performed on RLU data for the different incubations. A two-tailed Student's *t* test was used to analyse the statistical differences between different data points.

RESULTS

Biochemical characterization of hCTR2

To characterize hCTR2, hCTR1–vsvG and hCTR2–vsvG were expressed in HEK-293T cells, immunoprecipitated and subjected to immunoblot analysis. No precipitated proteins were detected in cells transfected with the empty vector, whereas hCTR1–vsvG was observed to migrate on SDS/PAGE at approx. 35 kDa (Figure 1B). This was consistent with previous studies [15], which indicated that the fully glycosylated mature hCTR1 was expressed. hCTR2–vsvG was detected to migrate with an apparent molecular mass of approx. 17 kDa (Figure 1B), in agreement with its size as predicted from amino acid sequence analysis (17 000 Da). Crude cell fractionation studies indicated that hCTR2 was associated with cellular membranes (results not shown). This biochemical analysis indicated that hCTR2–vsvG was expressed as a stable membrane-associated protein and was most probably not glycosylated.

Chemical cross-linking and two-dimensional crystallography experiments conducted previously revealed that hCTR1 assembles as a trimer [16,18]. Thus we considered the possibility that hCTR2 also exists as an oligomeric complex. The amine-reactive chemical cross-linker EGS was used to covalently link cellular interacting proteins. Chemical cross-linking with EGS in HEK-293T cells transiently transfected with hCTR2–vsvG resulted in the detection of discrete vsvG immunopositive bands which migrated at apparent molecular masses of approx. 24 and 35 kDa. The intensity of these putative hCTR2–vsvG oligomers increased in an EGS concentration-dependent manner (Figure 1C; arrows). At high EGS concentrations (1 mM), additional complexes of even higher molecular mass (> 200 kDa) were also observed (results not shown). These results suggested that hCTR2 may be capable of forming oligomeric complexes, similar to those observed for hCTR1 [16].

To investigate further this possibility, hCTR2 constructs were generated with a FLAG tag present at the C-terminus. These constructs were co-expressed with hCTR2–vsvG in HEK-293T cells, and cell lysates were subjected to co-immunoprecipitation with either anti-FLAG M2–agarose beads or Protein A–agarose beads coupled to rabbit anti-vsvG antibodies. Immunoprecipitation of both vsvG-tagged proteins (Figure 1D, lanes 7–9) and FLAG-tagged proteins (Figure 1D, lanes 4–6) was observed. Co-immunoprecipitation of hCTR2–vsvG with hCTR2–FLAG was observed (Figure 1D, lane 1), but no interaction was noted with RabIP4–vsvG (Figure 1D, lane 2) or with cullin1–FLAG (Figure 1D, lane 3), which were used as negative controls. Taken together, these experiments suggest that hCTR2 monomers mutually interact, and support the hypothesis that CTR proteins form trimeric complexes to enable copper transport.

Intracellular localization of hCTR2

To investigate the cellular localization of hCTR2, we generated constructs encoding hCTR2 with a C-terminal eGFP tag. Similarly to hCTR2–vsvG, hCTR2–eGFP expressed in HEK-293T cells also migrated at its expected molecular mass of 40 kDa and could be detected in higher-molecular-mass oligomers (results not shown). The cellular localization of hCTR2 was determined after transient transfection of hCTR2–eGFP into HEK-293T cells, U2OS cells and HeLa cells (Figure 2A). hCTR2–eGFP was not detected at the plasma membrane, but was primarily localized in relatively large vesicles in all three cell types (Figure 2A). We set out to exclude the possibility that the inserted tag could have interfered with the localization of transiently expressed hCTR2. Independently transfected hCTR2–vsvG and hCTR2–FLAG were also detected in large vesicular compartments in multiple cell types (results not shown), and co-expression of hCTR2–vsvG with hCTR2–eGFP resulted in strong co-localization between the two constructs (Figure 2B). The latter result indicates that the cellular localization of hCTR2 was independent of the tag added to the protein.

Consistent with previous results, hCTR1–eGFP was detectable in HeLa cells at the plasma membrane, but was primarily localized in intracellular vesicles, and hCTR1-eGFP also partly co-localized with hCTR2 (Figure 3A) [15,16]. Cell-surface hCTR1 is known to be rapidly and specifically internalized upon incubation of HEK-293T cells with increasing concentrations of copper [17]. To determine whether copper affects hCTR2 localization, HEK-293T cells were transiently transfected with hCTR2–eGFP. Cells were incubated with different copper concentrations or with the copper-chelating agent, BCS, for 1 h. No apparent copper-dependent relocalization of hCTR2 was observed (Figure 3B), which is in accordance with previous results suggesting that the intracellular fraction of hCTR1 does not undergo copper-dependent relocalization [15].

The nature of the vesicular localization of hCTR2 in HEK-293T cells was investigated further. HEK-293T cells were transiently transfected with hCTR2–eGFP, and immunofluorescence labelling of different cellular marker proteins was performed. No significant co-localization was observed between hCTR2–eGFP and TfR, an early endosomal marker, or between hCTR2–eGFP and p230, a TGN-resident protein (Figure 4). However, hCTR2 was partly co-localized with late endosomes, identified by labelling with an anti-CD63 antibody, and marked co-localization was observed with the lysosomal markers LAMP-1 and LAMP-2 (Figure 4, arrowheads). Similar results were observed in HeLa cells (results not shown), indicating that the localization of hCTR2 in late endosomes and lysosomes was not cell-type-specific.

A novel transcription-based copper sensor to measure cytosolic bioavailable copper pools

To address whether hCTR2 could facilitate copper uptake, a novel transcription-based copper biosensor was designed. The design of this sensor was based on the endogenous capacity of cells to transactivate metallothionein genes in response to elevated cytosolic copper availability. An increase in the concentration of copper in the cytosol results in the displacement of zinc from metallothioneins. The released zinc binds to and activates MTF (metal responsive transcription factor)-1, which subsequently induces gene expression by binding to MREs in the promoter region of specific genes [7,35]. Four MREs from the murine metallothionein 1A promoter [7,32] were cloned upstream of

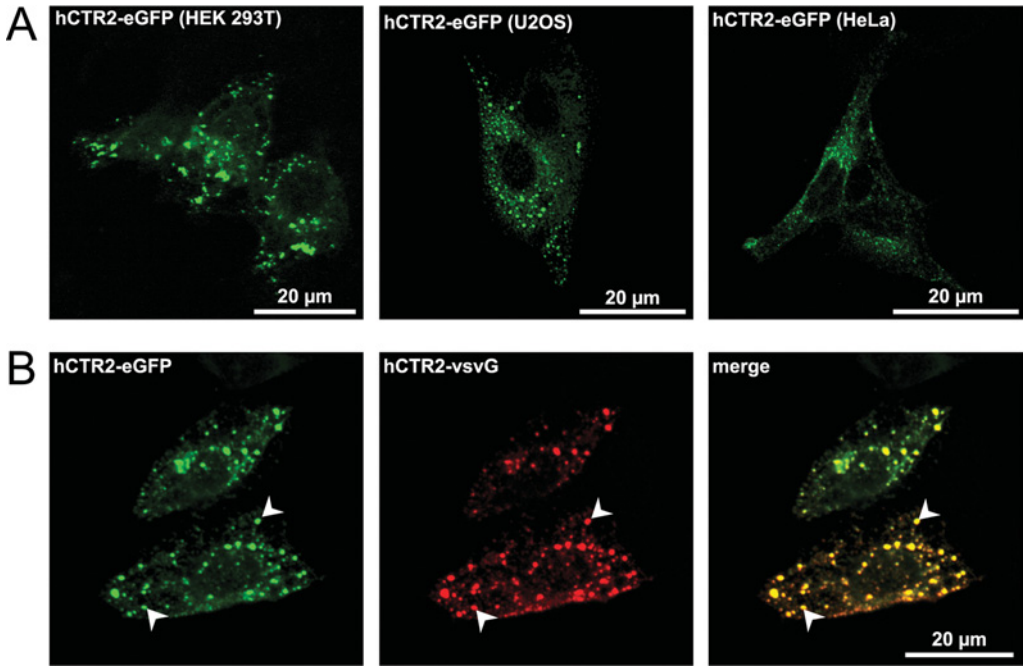

Figure 2 hCTR2 is localized in intracellular vesicles

(**A**) Localization of hCTR2 was assessed by direct confocal laser-scanning microscopy in HEK-293T, U2OS and HeLa cells after transient transfection with hCTR2–eGFP. (**B**) HeLa cells were transiently co-transfected with both hCTR2–vsvG and hCTR2–eGFP constructs. hCTR2–vsvG was immunolabelled with rabbit anti-vsvG antibodies, and secondary labelling was performed with Alexa Fluor® 568 conjugated-goat anti-rabbit and goat anti-mouse antibodies. hCTR2–eGFP was visualized by direct confocal microscopy. Co-localization is indicated by arrowheads.

the firefly luciferase open reading frame in the pGL3-E1b-TATA vector (Figure 5A), and this resulted in the formation of the MRE–luciferase reporter. A construct encoding the metal-insensitive TK (thymidine kinase)–*Renilla* luciferase was used to correct for differences in transfection efficiencies. Similarly to the endogenous metallothionein 1A promoter, the MRE–luciferase reporter was predicted to be transactivated in a metal-concentration-dependent fashion by MTF-1 [7]. In this way, the MRE–luciferase reporter measured bioavailable cytosolic copper. To test the validity of this approach, the MRE–luciferase reporter was transiently transfected into HEK-293T cells (Figure 5C) and U2OS cells (results not shown), and cells were incubated with different copper concentrations for 24 h. At the concentration of copper normally present in the medium, reporter activity was slightly increased compared with cells transfected with a control vector containing no MREs. A linear concentration-dependent induction of the activity of the MRE–luciferase reporter was noted when cells were incubated with 20–100 μM $CuCl_2$, an effect that was not observed in cells transfected with the empty vector only (Figure 5C). The induction of the MRE–luciferase reporter activity was approx. 5-fold increased at a concentration of 100 μM $CuCl_2$, in comparison with the activity observed at the concentration of basal copper present in the medium. Higher concentrations of copper did not result in further induction of MRE–luciferase reporter activity. A more detailed examination of MRE–luciferase reporter activities at low copper concentrations revealed that the sensor was not effectively induced by copper concentrations below 20 μM in these cells (results not shown). Since the reporter is responsive to cytosolic copper, an increase in reporter activity was interpreted as an indication that copper import and transport across a cellular membrane had occurred. Quantitative RT (reverse transcription)–PCR experiments revealed that induction of the endogenous metallothionein 1A promoter also occurred at the same copper concentrations as the MRE–luciferase reporter activity was induced (results not shown). As different metals are known to induce MTF-1-mediated transcription [7], the specificity of the MRE–luciferase reporter for several other biologically important metals was tested. Zinc is especially relevant in this respect, since activation of MTF-1 is caused by incorporation of cellular zinc into MTF-1 after displacement of zinc from metallothioneins by other metals, such as copper [7]. Initially, metal toxicity was determined by MTT viability assays to calculate LD_{50} values in our cells (Figure 5B). Subsequently, HEK-293T cells were transiently transfected with the MRE–luciferase reporter, and, 24 h after transfection, cells were incubated with either a low or a high metal concentration that was still below the lethal concentration (Figure 5D). $CuCl_2$ and $ZnCl_2$ resulted in the induction of reporter activities in a concentration-dependent manner, whereas $MgCl_2$, $FeCl_3$ and $MnCl_2$ failed to activate the MRE–luciferase reporter. MTF-1-mediated transcription may also be induced by other factors, such as oxidative stress and hypoxia [7,36]. However, no MRE–luciferase reporter induction was observed as a result of oxidative stress. This was examined by incubation of transfected cells with 100 μM hydrogen peroxide or 100 μM paraquat for 24 h (results not shown) [37]. To mimic hypoxia, cells were treated with DFO [38], which resulted in the induction of the hypoxia-responsive 5× HRE reporter (Figure 5E). The MRE–luciferase reporter activity was only slightly induced upon DFO treatment, whereas $CuCl_2$ strongly induced the MRE reporter, but not the 5× HRE reporter (Figure 5D). Considered together with the idea that all experiments in the present study were performed under normoxic conditions, we concluded that the MRE–luciferase reporter specifically detects elevated copper and zinc concentrations under these defined experimental conditions.

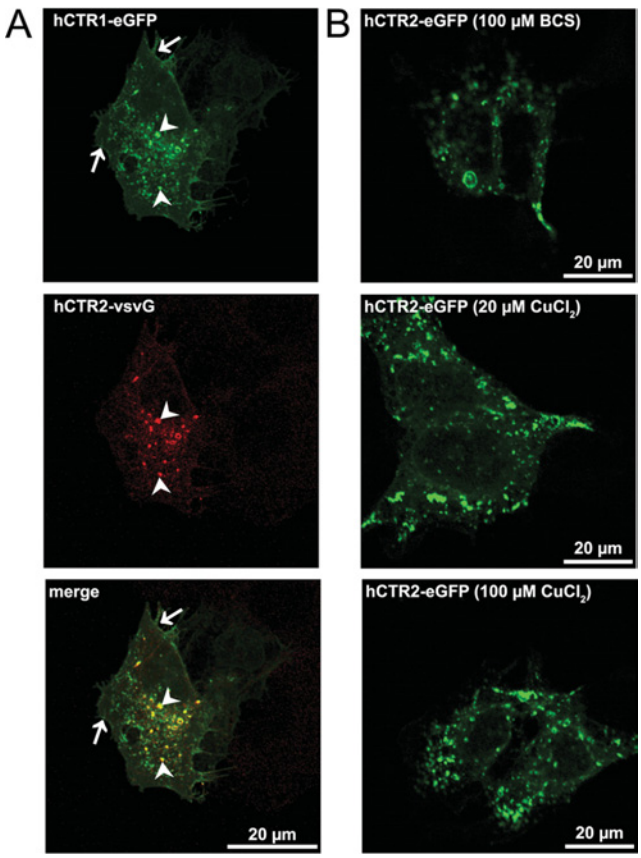

Figure 3 hCTR2 is partially co-localized with hCTR1

(**A**) Confocal laser-scanning microscopy was performed on HeLa cells which were transiently transfected with hCTR1–eGFP and hCTR2–vsvG constructs. hCTR2–vsvG was immunolabelled with rabbit anti-vsvG antibodies, and secondary labelling was performed using Alexa Fluor® 568-conjugated antibodies. hCTR1–eGFP was visualized by direct confocal microscopy. Plasma membrane localization of hCTR1–eGFP is indicated with arrows, and co-localization with arrowheads. (**B**) HEK-293T cells were transiently transfected with the hCTR2–eGFP construct. Prior to analysis, cells were incubated for 1 h with either BCS or $CuCl_2$ at the concentrations indicated.

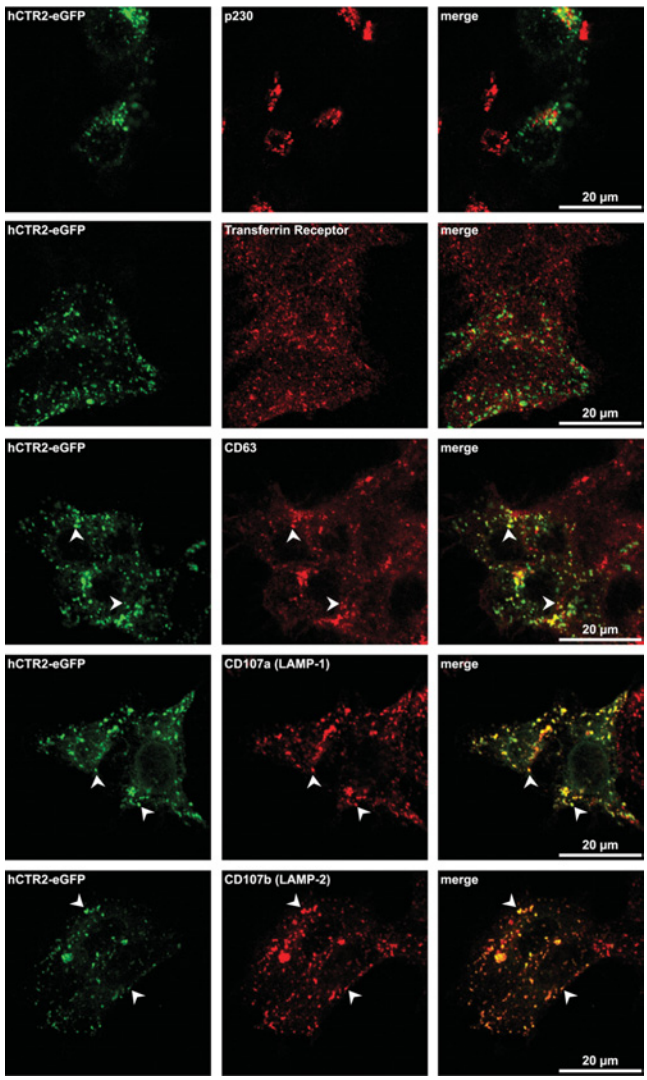

Figure 4 hCTR2 co-localized with late endosomal and lysosomal vesicles

HEK-293T cells were transiently transfected with hCTR2–eGFP prior to labelling with antibodies against different vesicular markers: the TGN marker p230, TfR (early endosomal marker), CD63 (late endosomal marker) and the lysosomal markers LAMP-1 and LAMP-2. Secondary labelling was performed using Alexa Fluor® 568-conjugated antibodies before being visualized by direct confocal microscopy. Green and red channels were merged to determine the co-localization of hCTR2–eGFP with the different compartmental markers (arrowheads).

hCTR1 and hCTR2 both facilitate copper uptake

Next, we tested whether this approach could be used to effectively assess perturbations in the known copper import pathway. To investigate this, hCTR1–FLAG was co-transfected into HEK-293T cells together with the MRE–luciferase reporter. Without supplementing the medium with additional $CuCl_2$, this resulted in a significant increase (approx. 3-fold) in reporter activity when compared with cells transfected with the empty vector (Figures 6A and 6B). This increase in reporter activity could be prevented completely by incubation with the copper chelator, BCS (results not shown), indicating that exogenous expression of hCTR1–FLAG resulted in a significant increase in the cytosolic copper concentration in the presence of cell culture medium containing a low concentration of copper. Addition of $CuCl_2$ (up to 2.5 μM) resulted in a marked and significant increase in the reporter activity, with a maximal 10-fold induction observed at 2.5 μM $CuCl_2$ (Figure 6A). Since the MRE–luciferase reporter was activated by zinc as well as by copper, one possible explanation for the reporter induction is that exogenous expression of hCTR1–FLAG resulted in the mobilization of sequestered vesicular zinc pools under conditions of excess cytosolic copper. To address this possibility, the effects of transient transfection of hCTR1–FLAG on zinc-induced reporter activity were assessed. In transfected cells containing the empty vector, no induction of the MRE–luciferase reporter activity was observed when incubated with $ZnCl_2$ at the same concentrations as used in the copper experiments. In cells expressing exogenous hCTR1–FLAG, the basal reporter activity was raised approx. 3-fold as shown above (Figures 6A and 6B), but the MRE–luciferase reporter activity was not induced further as a result of additional $ZnCl_2$ (Figure 6B). These results strongly indicate that expression of hCTR1–FLAG resulted in an increase in the bioavailability of copper, but not zinc. As a control, immunoblot analysis of hCTR1–FLAG was used to determine protein expression under these conditions (Figure 6E). Together, these data indicated the feasibility of using the MRE–luciferase reporter to specifically assess changes in the expression of copper import proteins on copper uptake. Furthermore, these results confirmed previous observations that the expression of hCTR1 was a limiting factor in copper import, at least at relatively low copper concentrations [14].

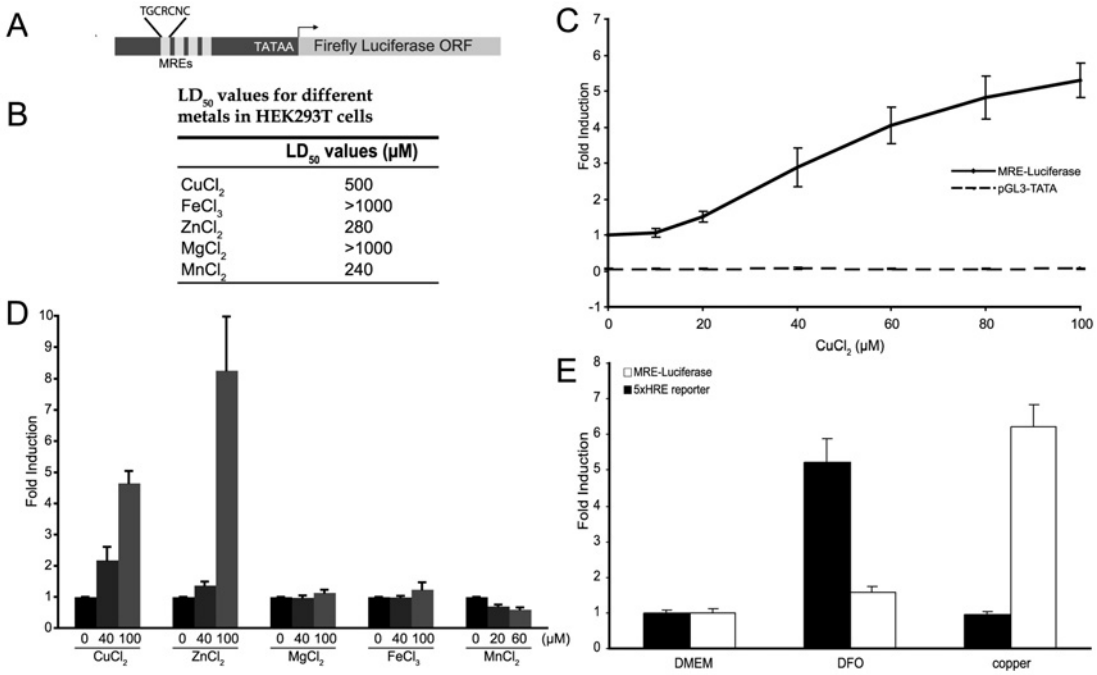

Figure 5 Characterization of a novel MRE–luciferase reporter assay

(**A**) The MRE–luciferase reporter was constructed by cloning four MREs upstream of the firefly luciferase open reading frame of the pGL3-TATA construct as indicated. (**B**) HEK-293T cells were transiently transfected with the MRE–luciferase reporter or the control vector, pGL3-TATA. After transfection, cells were incubated for 24 h with different concentrations of $CuCl_2$. (**C**) Metal toxicity was measured using MTT viability assays after incubation for 24 h with different metal concentrations, and LD_{50} values were also determined. (**D**) HEK-293T cells were transiently transfected with the MRE–luciferase reporter, and, 24 h after transfection, cells were incubated with a low or a high sub-lethal metal concentration. (**E**) HEK-293T cells were transiently transfected with either the MRE–luciferase reporter or a HRE–luciferase reporter. After transfection, cells were incubated with 100 μM $CuCl_2$ or 100 μM of DFO (to mimic hypoxia). Luciferase reporter activities were measured and normalized for *Renilla* luciferase activities. Values are expressed as fold induction relative to control incubations $\pm$S.E.M. (see the Experimental section) ($n \geqslant 3$).

Next, the potential role of hCTR2 in copper import was studied in a similar manner to that of hCTR1 by co-transfection of hCTR2–FLAG and MRE–luciferase reporter in HEK-293T cells. Expression of hCTR2–FLAG was verified by immunoblot analysis (Figure 6E). In cells transfected with the empty vector, reporter activity was induced in the presence of 10–20 μM $CuCl_2$ (results not shown). However, hCTR2–FLAG expression resulted in a significantly higher reporter induction compared with cells transfected with the empty vector. At concentrations of 40 and 100 μM $CuCl_2$, expression of hCTR2–FLAG resulted in a >2-fold increase (Figure 6C). The increased hCTR2–FLAG-dependent MRE–luciferase reporter activation was copper-specific, as no differences were observed on incubation with $ZnCl_2$ (Figure 6D). To demonstrate further that the function of hCTR2 was copper-specific, we mutated the methionine residues in the MXXXM motif to isoleucine. Previous findings by Eisses and Kaplan [25] revealed a marked reduction in hCTR1-mediated copper uptake after disruption of the analogous methionine residues present in the MXXXM motif of hCTR1. Whereas expression of wild-type hCTR1–FLAG or hCTR2–FLAG resulted in a significant copper-dependent induction of the MRE–luciferase reporter, substitution of the MXXXM motif to IXXXI completely abolished the induction of the reporter by hCTR1–FLAG and by hCTR2–FLAG (Figures 6A and 6C). The lack of induction was a result of the amino acid substitution, as all the constructs were shown to be expressed successfully (Figure 6E). No differences were observed after incubation with $ZnCl_2$ (Figures 6B and 6D). Taken together, expression of hCTR2 facilitates cellular copper uptake with a lower affinity compared with hCTR1.

DISCUSSION

Since the initial characterization of hCTR1 almost a decade ago [30], elegant studies have addressed the structure and localization of mammalian Ctr1, its transport kinetics, regulation by copper and the role in embryonic development and dietary copper uptake in mice [14–18,20–27,29,39,40]. Although these studies have greatly increased our knowledge of the mechanisms of cellular copper uptake, they also established that Ctr1-independent copper import pathways exist. MEFs obtained from *Ctr1*-knockout embryos displayed low-affinity copper uptake [23]. On the basis of the evidence of the present study, we propose that hCTR2, a protein with structural similarity to hCTR1, but with a previously unknown function, mediates an alternative low-affinity copper import pathway in human cells.

To be able to characterize the function of hCTR2, we constructed a novel metal sensor. This sensor allowed sensitive and high-throughput assessment of copper homoeostasis. It is important to note that the MRE–luciferase reporter measures cytosolic bioavailable copper and was based on a cell-intrinsic copper-sensing mechanism, removing the need to add exogenous compounds that bind copper directly and might potentially interfere with the copper homoeostatic mechanisms present in the cell [41]. By performing control experiments using zinc, the sensor allowed determination of the specific effects of exogenously expressed proteins on copper metabolism. Our data strongly indicated that hCTR2 facilitates cellular copper import with a lower affinity than that mediated by hCTR1. At copper concentrations below 10 μM, at which hCTR1-dependent MRE–luciferase reporter activity was maximally induced, no effect of hCTR2

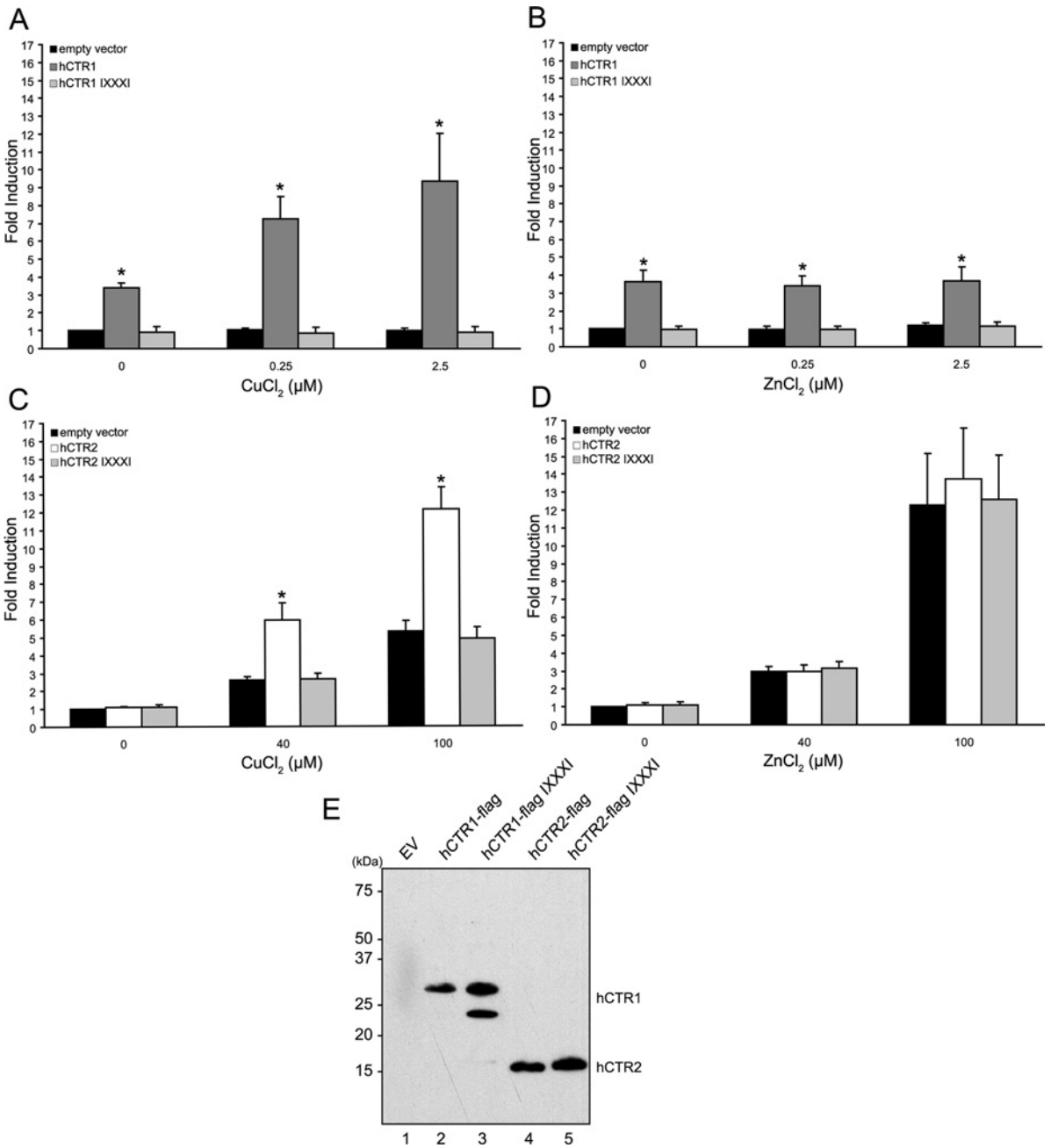

Figure 6 Cellular copper uptake is facilitated by hCTR2 and is dependent on the CTR-specific MXXXM motif

The MXXXM motifs were mutated to form IXXXI in pEBB-hCTR1-FLAG and pEBB-hCTR2-FLAG. HEK-293T cells were transiently transfected with the MRE–luciferase reporter in combination with wild-type pEBB-hCTR1-FLAG (**A**,**B**), pEBB-hCTR2-FLAG (**C**,**D**) or the IXXXI mutant motif constructs. After transfection, cells were incubated for 24 h with increasing amounts of $CuCl_2$ (**A**,**C**) or $ZnCl_2$ (**B**,**D**). MRE–luciferase reporter activities were measured and RLU were calculated after normalization for *Renilla* luciferase activity. Values are expressed as fold induction relative to control incubations (see the Experimental section) $\pm$ S.E.M. ($n = 3$). Statistical differences between empty vector (EV)- and hCTR1- or hCTR2-transfected cells are indicated ($^*P < 0.01$). (**E**) Lysates from the MRE–luciferase assay were resuspended in SDS/PAGE sample buffer, resolved by SDS/PAGE and subjected to immunoblot analysis using the mouse anti-FLAG antibody. Molecular masses are indicated in kDa.

expression on reporter activity could be detected. In contrast, exogenous expression of hCTR2 resulted in significantly higher copper-dependent MRE–luciferase activity compared with empty vector controls. This effect was copper-specific, since mutation of conserved methionine residues known to be essential for copper transport in CTR proteins completely abolished the activation of the reporter. Therefore hCTR2 expression resulted in a specific increase in cytosolic copper availability at high concentrations of copper in the extracellular medium. Since the copper sensor does not measure the transport of copper directly, further studies are necessary to address the kinetics of hCTR2-mediated copper import in more detail.

The apparent steady-state localization of this protein in the endosomal and lysosomal compartments is notable. Lysosomes in mammalian cells and vacuoles in yeast have equivalent functions. In *Saccharomyces cerevisiae*, the hCTR2 orthologue, yCtr2p, is

localized to the vacuolar membrane and can mobilize vacuolar copper pools [42]. A similar vacuolar membrane localization was observed for Ctr6, the hCTR2 orthologue in the fission yeast, *Schizosaccharomyces pombe* [43]. Combined with our data, we suggest that the endosomal and lysosomal localization and mobilization of intracellular copper stores are common properties of yeast and mammalian CTR2/Ctr6 proteins. Our data suggest that the observed intracellular localization of hCTR2 is correct, since it was observed in multiple cell types and appeared to occur independently of the tags present. Moreover, expressed proteins were demonstrated to stimulate functional copper uptake activity. A similar localization of endogenous CTR2 in large vesicular compartments, reminiscent of late endosomes and lysosomes, was observed in human and monkey cells in other independent studies (J. Bertinato, personal communication). There is ample precedence for the localization of CTRs in intracellular compartments. Under basal copper levels, ATP7A resides in the Golgi-network and is only distributed towards peripheral vesicles and the plasma membrane in response to an increase in cytosolic copper concentrations [44,45]. In addition, hCTR1 also resides predominantly in intracellular vesicles, but has been shown to recycle constitutively between this vesicular compartment and the plasma membrane [17,24]. In fact, part of the intracellular pool of hCTR2 resided in vesicular compartments that also contained hCTR1, but further studies are required to clarify the implications of this intriguing observation.

Our results suggest that hCTR2 is an intracellular oligomeric membrane protein which is rate-limiting for the delivery of copper into the cytosol at high copper concentrations. We have proposed a model of cellular copper uptake by hCTR2. In mammalian cells, extracellular copper and cuproenzymes destined for lysosomal degradation may be endocytosed or pinocytosed by CTR-dependent or -independent mechanisms. Copper may subsequently be concentrated into lysosomes, prior to mobilization by hCTR2. This process may require high extracellular concentrations of copper or prolonged concentration of copper in lysosomal vesicles, consistent with our observation that hCTR2 stimulates copper uptake at relatively high copper concentrations. This model fits with the current knowledge of the biology of dietary copper import and intracellular copper sequestration. Intestinal epithelium of gut-specific *Ctr1*-null mice unexpectedly accumulated dietary copper [22]. The failure to express Ctr1 did not lead to reduced cellular copper uptake, but rather caused an increase in the intracellular sequestration of copper, presumably in lysosomal vesicles. If mouse Ctr2 could function to mobilize copper from intracellular pools in gut epithelium, this activity is clearly not sufficient to prevent the severe systemic copper deficiency present in intestine-specific *Ctr1*-null mice [22]. Although the existence of vesicular copper stores in mammalian cells remains speculative, extensive copper accumulation has indeed been observed in lysosomes of Wilson disease patients [46], in LEC (Long-Evans Cinnamon) rats (a model for Wilson disease) [47] and in the liver cells of Bedlington terriers affected with copper toxicosis [48]. Finally, several other metal transport systems utilize the endocytic machinery to import metals into the cytosol. In yeast, zinc transporters regulate vacuolar zinc stores to modulate zinc homoeostasis [49]. The mouse zinc transporters ZIP1, ZIP3 and ZIP4 are localized in intracellular vesicles, and may translocate to the plasma membrane to allow zinc uptake [50,51]. Furthermore, the DMT (divalent metal transporter) 1 protein is involved in the transfer of endocytosed iron into the cytosol [52,53]. Therefore cellular copper uptake may require a combination of transport across the plasma membrane, endocytosis of the metal and mobilization from intracellular pools, as observed for the uptake of other transition metals.

In summary, these results suggest that hCTR2 is predominantly localized in the endosomal system and stimulates copper uptake with a relatively low affinity to make it bioavailable in the cytosol, and suggest that hCTR2 may be responsible for the residual copper uptake activity observed in cells obtained from *Ctr1*-null embryos. Since this work is the first study on the function and localization of hCTR2, many questions remain unanswered. It will be important to examine further the nature and function of vesicular copper sequestration in copper homoeostasis, and to identify the mechanisms that are responsible for import of copper into endosomes and lysosomes. Ultimately, studying the impact on copper homoeostasis of knocking out *Ctr2* from the mouse genome at the level of the entire organism will be required to obtain a complete understanding of the regulation of copper uptake under different conditions and cellular demands.

We thank Dr Walter Schaffner for providing the 4 × MRE(d) construct, and Dr P.J. van de Sluijs for providing the pCL-NEO Rablp4-vsvG construct. We are grateful to Dr Eric Kalkhoven and Professor Dr Cisca Wijmenga for critical evaluation of the manuscript, and the members the Klomp–Wijmenga group for valuable discussions and assistance. This work was supported by a grant from the Netherlands Organization for Scientific Research (NWO: 912-04-106).

REFERENCES

1 Culotta, V. C., Lin, S. J., Schmidt, P., Klomp, L. W., Casareno, R. L. and Gitlin, J. (1999) Intracellular pathways of copper trafficking in yeast and humans. Adv. Exp. Med. Biol. **448**, 247–254
2 de Bie, P., van de Sluis, B., Klomp, L. and Wijmenga, C. (2005) The many faces of the copper metabolism protein MURR1/COMMD1. J. Hered. **96**, 803–811
3 Himelblau, E. and Amasino, R. M. (2000) Delivering copper within plant cells. Curr. Opin. Plant Biol. **3**, 205–210
4 Rae, T. D., Schmidt, P. J., Pufahl, R. A., Culotta, V. C. and O'Halloran, T. V. (1999) Undetectable intracellular free copper: the requirement of a copper chaperone for superoxide dismutase. Science **284**, 805–808
5 Casareno, R. L., Waggoner, D. and Gitlin, J. D. (1998) The copper chaperone CCS directly interacts with copper/zinc superoxide dismutase. J. Biol. Chem. **273**, 23625–23628
6 Hamza, I., Schaefer, M., Klomp, L. W. and Gitlin, J. D. (1999) Interaction of the copper chaperone HAH1 with the Wilson disease protein is essential for copper homeostasis. Proc. Natl. Acad. Sci. U.S.A. **96**, 13363–13368
7 Zhang, B., Georgiev, O., Hagmann, M., Gunes, C., Cramer, M., Faller, P., Vasak, M. and Schaffner, W. (2003) Activity of metal-responsive transcription factor 1 by toxic heavy metals and H_2O_2 *in vitro* is modulated by metallothionein. Mol. Cell. Biol. **23**, 8471–8485
8 Mercer, J. F., Livingston, J., Hall, B., Paynter, J. A., Begy, C., Chandrasekharappa, S., Lockhart, P., Grimes, A., Bhave, M., Siemieniak, D. et al. (1993) Isolation of a partial candidate gene for Menkes disease by positional cloning. Nat. Genet. **3**, 20–25
9 Vulpe, C., Levinson, B., Whitney, S., Packman, S. and Gitschier, J. (1993) Isolation of a candidate gene for Menkes disease and evidence that it encodes a copper-transporting ATPase. Nat. Genet. **3**, 7–13
10 Mendelsohn, B. A., Yin, C., Johnson, S. L., Wilm, T. P., Solnica-Krezel, L. and Gitlin, J. D. (2006) Atp7a determines a hierarchy of copper metabolism essential for notochord development. Cell Metab. **4**, 155–162
11 Petris, M. J. (2004) The SLC31 (Ctr) copper transporter family. Pflügers Arch. **447**, 752–755
12 Dancis, A., Yuan, D. S., Haile, D., Askwith, C., Eide, D., Moehle, C., Kaplan, J. and Klausner, R. D. (1994) Molecular characterization of a copper transport protein in *S. cerevisiae*: an unexpected role for copper in iron transport. Cell **76**, 393–402
13 Knight, S. A., Labbe, S., Kwon, L. F., Kosman, D. J. and Thiele, D. J. (1996) A widespread transposable element masks expression of a yeast copper transport gene. Genes Dev. **10**, 1917–1929
14 Eisses, J. F. and Kaplan, J. H. (2002) Molecular characterization of hCTR1, the human copper uptake protein. J. Biol. Chem. **277**, 29162–29171
15 Klomp, A. E., Tops, B. B., Van Denberg, I. E., Berger, R. and Klomp, L. W. (2002) Biochemical characterization and subcellular localization of human copper transporter 1 (hCTR1). Biochem. J. **364**, 497–505
16 Lee, J., Pena, M. M., Nose, Y. and Thiele, D. J. (2002) Biochemical characterization of the human copper transporter Ctr1. J. Biol. Chem. **277**, 4380–4387

17 Petris, M. J., Smith, K., Lee, J. and Thiele, D. J. (2003) Copper-stimulated endocytosis and degradation of the human copper transporter, hCtr1. J. Biol. Chem. **278**, 9639–9646

18 Aller, S. G. and Unger, V. M. (2006) Projection structure of the human copper transporter CTR1 at 6-Å resolution reveals a compact trimer with a novel channel-like architecture. Proc. Natl. Acad. Sci. U.S.A. **103**, 3627–3632

19 Nose, Y., Rees, E. M. and Thiele, D. J. (2006) Structure of the Ctr1 copper trans'PORE'ter reveals novel architecture. Trends Biochem. Sci. **31**, 604–607

20 Lee, J., Prohaska, J. R. and Thiele, D. J. (2001) Essential role for mammalian copper transporter Ctr1 in copper homeostasis and embryonic development. Proc. Natl. Acad. Sci. U.S.A. **98**, 6842–6847

21 Kuo, Y. M., Gybina, A. A., Pyatskowit, J. W., Gitschier, J. and Prohaska, J. R. (2006) Copper transport protein (Ctr1) levels in mice are tissue specific and dependent on copper status. J. Nutr. **136**, 21–26

22 Nose, Y., Kim, B. E. and Thiele, D. J. (2006) Ctr1 drives intestinal copper absorption and is essential for growth, iron metabolism, and neonatal cardiac function. Cell Metab. **4**, 235–244

23 Lee, J., Petris, M. J. and Thiele, D. J. (2002) Characterization of mouse embryonic cells deficient in the ctr1 high affinity copper transporter. Identification of a Ctr1-independent copper transport system. J. Biol. Chem. **277**, 40253–40259

24 Klomp, A. E., Juijn, J. A., van der Gun, L. T., van den Berg, I. E., Berger, R. and Klomp, L. W. (2003) The N-terminus of the human copper transporter 1 (hCTR1) is localized extracellularly, and interacts with itself. Biochem. J. **370**, 881–889

25 Eisses, J. F. and Kaplan, J. H. (2005) The mechanism of copper uptake mediated by human CTR1: a mutational analysis. J. Biol. Chem. **280**, 37159–37168

26 Aller, S. G., Eng, E. T., De Feo, C. J. and Unger, V. M. (2004) Eukaryotic CTR copper uptake transporters require two faces of the third transmembrane domain for helix packing, oligomerization, and function. J. Biol. Chem. **279**, 53435–53441

27 Puig, S., Lee, J., Lau, M. and Thiele, D. J. (2002) Biochemical and genetic analyses of yeast and human high affinity copper transporters suggest a conserved mechanism for copper uptake. J. Biol. Chem. **277**, 26021–26030

28 Pena, M. M., Lee, J. and Thiele, D. J. (1999) A delicate balance: homeostatic control of copper uptake and distribution. J. Nutr. **129**, 1251–1260

29 Puig, S. and Thiele, D. J. (2002) Molecular mechanisms of copper uptake and distribution. Curr. Opin. Chem. Biol. **6**, 171–180

30 Zhou, B. and Gitschier, J. (1997) *hCTR1:* a human gene for copper uptake identified by complementation in yeast. Proc. Natl. Acad. Sci. U.S.A. **94**, 7481–7486

31 Mosmann, T. (1983) Rapid colorimetric assay for cellular growth and survival: application to proliferation and cytotoxicity assays. J. Immunol. Methods **65**, 55–63

32 Westin, G., Gerster, T., Muller, M. M., Schaffner, G. and Schaffner, W. (1987) OVEC, a versatile system to study transcription in mammalian cells and cell-free extracts. Nucleic Acids Res. **15**, 6787–6798

33 de Bie, P., van de Sluis, B., Burstein, E., Duran, K. J., Berger, R., Duckett, C. S., Wijmenga, C. and Klomp, L. W. (2006) Characterization of COMMD protein–protein interactions in NF-κB signalling. Biochem. J. **398**, 63–71

34 Shibata, T., Giaccia, A. J. and Brown, J. M. (2000) Development of a hypoxia-responsive vector for tumor-specific gene therapy. Gene Ther. **7**, 493–498

35 Palmiter, R. D. (1994) Regulation of metallothionein genes by heavy metals appears to be mediated by a zinc-sensitive inhibitor that interacts with a constitutively active transcription factor, MTF-1. Proc. Natl. Acad. Sci. U.S.A **91**, 1219–1223

36 Murphy, B. J., Andrews, G. K., Bittel, D., Discher, D. J., McCue, J., Green, C. J., Yanovsky, M., Giaccia, A., Sutherland, R. M., Laderoute, K. R. and Webster, K. A. (1999) Activation of metallothionein gene expression by hypoxia involves metal response elements and metal transcription factor-1. Cancer Res. **59**, 1315–1322

37 Poss, K. D. and Tonegawa, S. (1997) Reduced stress defense in heme oxygenase 1-deficient cells. Proc. Natl. Acad. Sci. U.S.A. **94**, 10925–10930

38 Bianchi, L., Tacchini, L. and Cairo, G. (1999) HIF-1-mediated activation of transferrin receptor gene transcription by iron chelation. Nucleic Acids Res. **27**, 4223–4227

39 Eisses, J. F., Chi, Y. and Kaplan, J. H. (2005) Stable plasma membrane levels of hCTR1 mediate cellular copper uptake. J. Biol. Chem. **280**, 9635–9639

40 Kuo, Y. M., Zhou, B., Cosco, D. and Gitschier, J. (2001) The copper transporter CTR1 provides an essential function in mammalian embryonic development. Proc. Natl. Acad. Sci. U.S.A. **98**, 6836–6841

41 Zeng, L., Miller, E. W., Pralle, A., Isacoff, E. Y. and Chang, C. J. (2006) A selective turn-on fluorescent sensor for imaging copper in living cells. J. Am. Chem. Soc. **128**, 10–11

42 Rees, E. M., Lee, J. and Thiele, D. J. (2004) Mobilization of intracellular copper stores by the ctr2 vacuolar copper transporter. J. Biol. Chem. **279**, 54221–54229

43 Bellemare, D. R., Shaner, L., Morano, K. A., Beaudoin, J., Langlois, R. and Labbe, S. (2002) Ctr6, a vacuolar membrane copper transporter in *Schizosaccharomyces pombe*. J. Biol. Chem. **277**, 46676–46686

44 Petris, M. J., Mercer, J. F., Culvenor, J. G., Lockhart, P., Gleeson, P. A. and Camakaris, J. (1996) Ligand-regulated transport of the Menkes copper P-type ATPase efflux pump from the Golgi apparatus to the plasma membrane: a novel mechanism of regulated trafficking. EMBO J. **15**, 6084–6095

45 Yamaguchi, Y., Heiny, M. E., Suzuki, M. and Gitlin, J. D. (1996) Biochemical characterization and intracellular localization of the Menkes disease protein. Proc. Natl. Acad. Sci. U.S.A. **93**, 14030–14035

46 Sternlieb, I., Van den Hamer, C. J., Morell, A. G., Alpert, S., Gregoriadis, G. and Scheinberg, I. H. (1973) Lysosomal defect of hepatic copper excretion in Wilson's disease (hepatolenticular degeneration). Gastroenterology **64**, 99–105

47 Terada, K., Aiba, N., Yang, X. L., Iida, M., Nakai, M., Miura, N. and Sugiyama, T. (1999) Biliary excretion of copper in LEC rat after introduction of copper transporting P-type ATPase, ATP7B. FEBS Lett. **448**, 53–56

48 Haywood, S., Fuentealba, I. C., Foster, J. and Ross, G. (1996) Pathobiology of copper-induced injury in Bedlington terriers: ultrastructural and microanalytical studies. Anal. Cell Pathol. **10**, 229–241

49 MacDiarmid, C. W., Gaither, L. A. and Eide, D. (2000) Zinc transporters that regulate vacuolar zinc storage in *Saccharomyces cerevisiae*. EMBO J. **19**, 2845–2855

50 Kim, B. E., Wang, F., Dufner-Beattie, J., Andrews, G. K., Eide, D. J. and Petris, M. J. (2004) Zn^{2+}-stimulated endocytosis of the mZIP4 zinc transporter regulates its location at the plasma membrane. J. Biol. Chem. **279**, 4523–4530

51 Wang, F., Dufner-Beattie, J., Kim, B. E., Petris, M. J., Andrews, G. and Eide, D. J. (2004) Zinc-stimulated endocytosis controls activity of the mouse ZIP1 and ZIP3 zinc uptake transporters. J. Biol. Chem. **279**, 24631–24639

52 Fleming, M. D., Romano, M. A., Su, M. A., Garrick, L. M., Garrick, M. D. and Andrews, N. C. (1998) Nramp2 is mutated in the anemic Belgrade (b) rat: evidence of a role for Nramp2 in endosomal iron transport. Proc. Natl. Acad. Sci. U.S.A. **95**, 1148–1153

53 Touret, N., Furuya, W., Forbes, J., Gros, P. and Grinstein, S. (2003) Dynamic traffic through the recycling compartment couples the metal transporter Nramp2 (DMT1) with the transferrin receptor. J. Biol. Chem. **278**, 25548–25557

Received 29 May 2007/4 July 2007; accepted 6 July 2007
Published as BJ Immediate Publication 6 July 2007, doi:10.1042/BJ20070705